Pergamon

Cement and Concrete Research 29 (1999) 1791–1797

CEMENT AND CONCRETE RESEARCH

Characterization of fly ash directly collected from electrostatic precipitator

Seung Heun Lee[a,*], Etsuo Sakai[b], Masaki Daimon[b], Wan Keun Bang[c]

[a]*Department of Materials Science and Engineering, Kunsan National University, 68 Miryong-dong, Kunsan, South Korea*
[b]*Department of Metallurgy and Ceramic Science, Graduate School, Tokyo Institute of Technology, 2-12-1 O-okayama Meguro-ku, Tokyo 152, Japan*
[c]*Department of Ceramic Engineering, Yonsei University, Seoul 120-749, South Korea*

Received 24 April 1997; accepted 20 July 1999

Abstract

Class-F fly ash was obtained from different hoppers at progressively farther distances from the boiler. Examinations showed that the ash collected from the farthest hopper tended to have finer particle size, greater density, lower carbon content, and higher glass content. When the boiler is operated at full load (600 MW) the glass content increased compared to half load (300 MW), but the Blaine specific surface area and carbon content decreased. Pozzolanic reactivity at 40°C is related to the fineness of the fly ash but the glass content has no significant influence on reactivity. There was a negative correlation between carbon content and the apparent viscosity of cement paste with fly ashes and 1.6% added superplasticizer.

Keywords: Fly ash; Characterization; Glass; Pozzolanic reactivity; Apparent viscosity

1. Introduction

In coal-fired power plants, coal ashes that pass through the combustion boiler are negatively charged by corona discharge in electrostatic precipitator (ESP) system. After attaching to the collection electrodes, these coal ashes are induced to fall into hoppers by action of rappers. ESP systems have many successive collection fields in the direction of flue gas travel. A hopper is installed in each collection field. In most coal-fired power plants, fly ashes collected from each hopper in the ESP system are transported and stored in a silo. However, the properties of the fly ashes collected from each hopper in an ESP system varies with the distance of the collection field from the boiler. The more distant hoppers get fly ash with larger Blaine specific surface areas [1]. Therefore, in ESP systems the hopper itself is expected to have the effect of classifying fly ashes.

Based on the above background, this research investigated physical and chemical properties of fly ashes collected from hoppers in an ESP system when the boiler was operated either at full load (600 MW) or at half load (300 MW). The effects of the character of fly ashes on their reactivity in calcium hydroxide mixtures was also investigated, and the influence of superplasticizer addition on the apparent of viscosity of cement paste with the fly ash was studied.

2. Methods

2.1. Materials

The fly ash used in the experiment came from a power plant in Japan that has been using Australian bituminous coal. Six samples of fly ash were collected from three different hoppers at each load. The load conditions of the boiler were 600 and 300 MW (at night). The locations of hoppers attached to the ESP system were named first, second, and third field in the direction of gas movement as shown Fig. 1. Reagent-grade $Ca(OH)_2$ was used to evaluate the reactivity of the fly ashes. Ordinary Portland cement (Blaine specific surface area, 356 m^2/kg; specific gravity, 3.15) and polycarboxylic acid superplasticizer were used to prepare paste samples for measurement of apparent viscosity.

2.2. Measurement of physical and chemical properties of fly ashes

The chemical properties of fly ashes, such as chemical composition, mineral composition, carbon content, loss on ignition, and adsorption amount of methylene blue (MB) were measured. The amount of MB adsorbed was determined by ultraviolet spectrometer. Solutions obtained by

* Corresponding author. Tel.: +82-654-469-4733; fax: +82-654-466-2086.

E-mail address: shlee@ks.kunsan.ac.kr (S.H. Lee)

0008-8846/99/$ – see front matter
PII: S0008-8846(99)00169-6

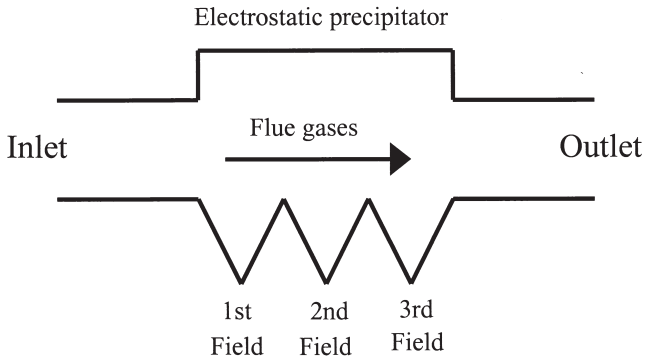

Fig. 1. The collected fields in the EPS.

filtering MB solution (25 mg/L) that had been added to 1 g of fly ash were used. Blaine specific surface area, particle size distribution (Microtrack-9320 HRA, USA), residue on 45-μm sieve, and specific gravity were measured to characterize physical properties of the fly ashes. Particle size distribution of fly ashes was measured by a laser diffraction method and color was observed visually.

Quantitative mineralogical compositions of fly ashes were obtained by internal standard method using powder X-ray diffraction analysis [2,3]. We used CaF_2 as the internal standard since it does not overlap with diffraction peaks of fly ash and it shows strong diffraction peaks. Aluminosilicate glass, having similar halo as that of glass phase in fly ash, was added as matrix. The X-ray diffraction pattern showed that the major crystalline phases were α-quartz and mullite and minor phases were magnetite and hematite. Therefore, calibration curves of α-quartz, mullite, magnetite, and hematite were prepared. The quartz, magnetite, and hematite used were reagent grade, and the mullite was prepared from high-purity sintered material. To reduce the mean deviation of the diffraction peak intensity, the samples were ground to 22 μm in size. Specimens with various compositions for calibration curves were made by mixing with aluminosilicate glass added to α-quartz, mullite (5–50 wt%), magnetite, and hematite (0.3–3.0 wt%). Calibration curves were obtained from X-ray diffraction patterns of the mixture with 20 wt% CaF_2 added. Table 1 lists the peaks and the ranges scanned for the various phase. The amount of glass was calculated by subtracting the amount of crystalline phases and the loss on ignition from the total amount.

An X-ray diffractometer (MAC-SCIENCE Co., Japan) with Cu target, operated at 40 KV and 30 mA, was used. The slit width divergency was 1 degree, and a 0.3-mm receiving slit with graphite monochrometer attached was used. The step-scanning method (0.02 degree) was used with 20-s preset time.

Table 1
X-ray diffraction peaks scanned for quanitative analysis

Phases	2θ	2θ range scanned
CaF_2	28.3	27.47–29.13
α-quartz	20.8	20.00–21.66
Mullite	16.4	15.57–17.23
Hematite	24.1	23.27–24.93
Magnetite	30.1	29.27–30.93

2.3. Measurement of the amount of reacted $Ca(OH)_2$

After fly ashes and $Ca(OH)_2$ were mixed at mole ratio of $Ca/(Si + Al) = 1$, water was added to pastes of water:powder weight fraction of 0.6. The pastes were reacted in incubator at 40°C for 3, 7, 28, and 56 days. The reacted sample were deposited in acetone for 1 day and dried at 110°C for 24 h. The amount of unreacted $Ca(OH)_2$ was determined by thermogravimetry and differential thermal analysis (TG-DTA) in a nitrogen atmosphere. The amount of reacted $Ca(OH)_2$ was obtained from this value and the loss on ignition.

2.4. Measurement of apparent viscosity

Fly ashes were mixed with ordinary Portland cement in 20 vol% and polycarboxylic acid plasticizer was added up to 2.0%. Pastes were then mixed at a volume fraction of 0.6. The viscosity of the pastes was measured at shear stress of 0 and 200 Pa at 20°C, using a rotary viscometer (Codix Co., Germany). The apparent viscosity value measured at 200 Pa was used.

3. Results and discussion

3.1. Fineness of fly ashes

The physical properties of fly ashes shown in Table 2 show that regardless of the boiler operating load, the Blaine specific surface area of fly ashes increases from the first field to the third one, with a value of more than 700 m^2/kg in the third field. The mean particle size of the fly ash was more than 30 μm in the first field, but was 6.9 μm in the third one. Most of fly ashes particles that were obtained in the third field passed through a 45-μm sieve. Fig. 2 shows the particle size distribution of fly ashes. From the curves it can be noticed that the maximum particle size of fly ashes becomes smaller, and the range of particle size distribution gets narrower, as distance from the boiler increases. Fly ashes in the first field represent multiple distributions with two maximum frequency diameters, but fly ashes in the third field show a normal distribution. With respect to differences in fineness with the operating boiler load, the fineness was slightly better at the half load of 300 MW than at full load of 600 MW. It can be inferred from the result that during half-load running of 300 MW, the amount of coal inserted into boiler was decreased to half in comparison with 600 MW; thus agglomeration by collision between pulverized coals during combustion was decreased.

3.2. Carbon content, loss on ignition, and adsorption of MB

Carbon content, loss on ignition, and amount of adsorption of MB are used to evaluate the amount of unburned carbon among fly ashes, as represented in Table 3. Carbon content and loss on ignition generally had low values, in the

Table 2
Physical properties of fly ashes

Fly ash	Load (MW)	Collected position	Specific gravity	Blaine value (m^2/kg)	Residue on 45 μm (%)	Mean particle size (μm)
A-1	600	First field	2.06	276	22.8	34.6
A-2	600	Second field	2.22	418	3.8	18.6
A-3	600	Third field	2.42	736	1.7	6.9
A′-1	300	First field	2.08	358	16.6	30.4
A′-2	300	Second field	2.23	498	3.2	15.6
A′-3	300	Third field	2.40	792	0.2	6.9

range of 0.3 to 1.5% and 1.1 to 2.1%. Carbon content was the least in case of the third-field fly ashes, with the smallest mean particle size, but loss on ignition had no such relationship. Fly ashes collected from the same place had less total carbon and lower loss on ignition at full load of 600 MW than at half load of 300 MW. This is due to the stable combustion state in full-load operation, which is appropriate to the capacity of the boiler. Since it has been reported that adsorption amount of MB is related to the adsorption amount of air-entraining agent on unburned carbon [4], the adsorption amount of MB was measured. However, in this experiment correlations among the adsorption amount of MB, carbon content, and loss on ignition were not evident because the carbon content of the fly ashes were all comparatively small. However, A′-1 and A′-2, with the most carbon content, had more loss on ignition and adsorption amount of MB.

3.3. Chemical and mineral characteristics of fly ashes

Table 4 represents the chemical compositions of the fly ashes. These represent typical composition of class-F fly ashes: analytical SiO_1 and Al_2O_3 were more than 85%, with low CaO value of 2.0 to 2.3%. With respect to variation in chemical composition with the place of collection, for fly ashes going from the first field to the third one analytical SiO_2 decreased by 3.5% at full load (600 MW) and 2.5% at half load (300 MW). But analytical Al_2O_3 increased to 1.6 and 1.5% in each run. The total amount of Fe_2O_3, alkali, and alkali earth oxides, which lower the melting temperature of coal ashes, was about 10% and increased slightly when going from the first field to the third field. There was only a slight difference in chemical composition with load change of the boiler.

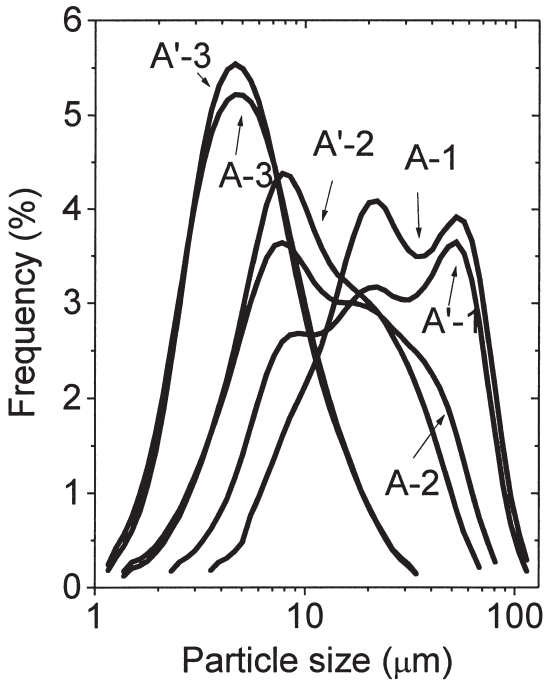

Fig. 2. Particle size distribution curves for fly ash.

Fig. 3 shows the results of X-ray diffraction of fly ashes. The major crystalline phases were mullite and alpha;-quartz and the minor crystalline phases were magnetite and hematite, regardless of the place of collection and the boiler load. Ca-containing phase could not be identified by X-ray diffraction analysis. As mentioned previously, the fly ashes used in this experiment had 2.3% or less CaO content, which is a low value, and most of the CaO in this range acts as modifiers during glass formation [5]. As shown in Fig. 3, the fly ashes contain a considerable amount of noncrystalline glass phase, and thus a series of halos attributed to glass phase appears. The halos indicate loss of long-range order. When the modifiers, alkali and alkali earth oxide, are introduced into random network structure, they break the network-creating nonbridging oxygen, which in turn leads to discontinuous structure. If the amount of modifiers increases, the structure becomes more discontinuous [1] and the position of maximum halo peak moves to high angle [6]. The position of maximum halo by X-ray diffraction was approximately to 2θ 23.3% for all of the fly ashes, and it may

Table 3
Carbon content and loss on ignition of fly ashes and adsorption amount of MB on fly ashes

Fly ash	Carbon content (%)	Loss on ignition (%)	Adsorption amount of MB (mg/g)
A-1	0.7	1.1	0.35
A-2	0.8	1.2	0.30
A-3	0.3	1.7	0.30
A′-1	1.5	2.1	0.50
A′-2	1.3	2.1	0.60
A′-3	0.4	1.8	0.30

Table 4
Chemical analysis of fly ashes (wt%)

Fly ash	SiO_2	Al_2O_3	Fe_2O_3	CaO	MgO	TiO_2	Na_2O	K_2O	SO_3	C
A-1	63.8	24.8	4.6	2.3	0.9	1.0	1.2	0.7	0.3	0.7
A-2	62.0	25.5	4.3	2.2	1.2	1.1	1.3	0.8	0.4	0.8
A-3	59.5	26.4	4.8	2.3	1.2	1.1	1.3	0.8	1.0	0.3
A′-1	62.5	26.4	4.2	2.0	1.1	1.1	1.2	0.8	0.5	1.5
A′-2	60.9	25.4	4.2	2.3	0.9	1.1	1.2	0.8	0.6	1.3
A′-3	59.6	26.4	4.3	2.3	1.1	1.1	1.4	0.8	1.0	0.4

be considered that they all have a basically similar glass structure.

Table 5 provides the mineral compositions as determined by quantitative powder X-ray diffraction. Contents of mullite, α-quartz, magnetite, and hematite were obtained directly by internal standard method. The glass content had the value in the range of 66.7 to 78.5%, and increased going from the first field to the third field. The amount of increase was 7.4% for 600 MW and 9.1% for 300 MW. At the same operating condition of the boiler, a higher glass content correlated with finer particles. The glass content depends on the rate of quenching. If the rate of quenching is faster, precipitation of crystalline phase is inhibited and the glass content is increased [7]. Ash particles are carried by flue gases generated from combustion, and particles exit the boiler. Because the minimum fluidizing velocities of particles depend largely on particle diameter rather than density, small particles have high velocities of minimum fluidizing [8]. Accordingly, fine particles have a higher rate of quenching. Fine fly ashes in the third field contain much more glass content and the glass content in 600 MW is higher than that of 300 MW. This may be attributed to the instability of combustion state following the decrease of the load. Using the mineralogical compositions for fly ashes and assigning exact stoichiometry to the crystalline phases, taking into account the presence of unburned carbon, calculations were made of the approximate compositions of the noncrystalline constituents of fly ashes. The chemical compositions of glasses were mainly composed of SiO_2 (63.3–67.6%) and Al_2O_3 (18.9–22.6%), which can form a network structure, and the modifier content was less than 10%. The Al/(Si + Al) mole ratio of the glass increased from 0.26 to 0.30 when going from the first field to the third field, regardless of operating load.

3.4. Specific gravity of fly ashes

The data in Table 2 include values for the apparent specific gravity of fly ashes. The values range from 2.06 for ash A-1, up to 2.42 for ash A-3. Some fly ash particles take the form of hollow spheres having lower value than the theoretical value of mineral compositions [1]. Fly ashes collected from the same location had similar values regardless of the boilder load, and they increased going from the first field to the third one. The specific gravity of fly ashes is expected to

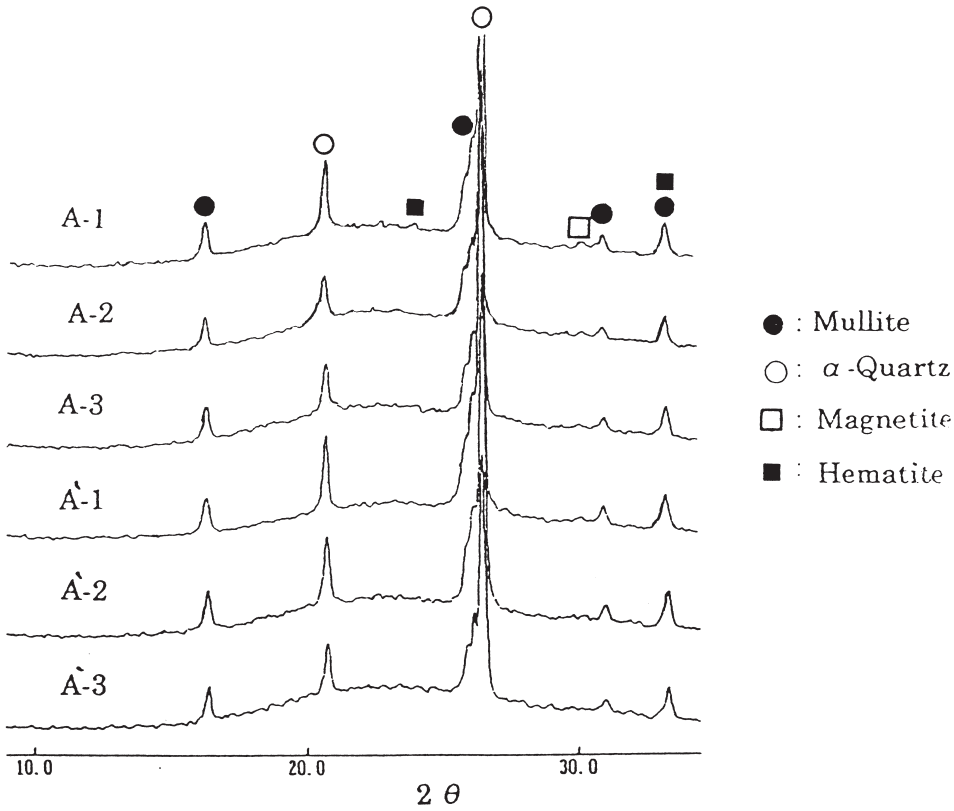

Fig. 3. X-ray diffraction patterns of fly ashes.

Table 5
Mineralogical compositions of fly ashes (wt%)

Fly ash	α-Quartz	Mullite	Hematite	Magnetite	Glass
A-1	10.9	15.4	0.6	0.9	71.1
A-2	8.7	12.4	–	0.4	77.3
A-3	7.2	12.6	–	–	78.5
A′-1	13.0	17.3	0.4	0.5	66.7
A′-2	11.3	16.5	–	0.4	69.7
A′-3	8.5	13.5	–	0.4	75.8

decrease from the standpoint of the mass proportions because the finer the particles are, the more likely the glass content of low specific gravity will increase. However, conflicting with the results of the experiment, the mineralogical compositions may not greatly affect the specific gravity. In considering the relation between carbon content and specific gravity, it should be noted that the carbon contents are less than 1%, and the specific gravity and carbon content do not have any correlation. Thus, the specific gravity may not be affected by porous particles such as charcoal. Hollow fine fly ash particles may have thick shell walls, because the finer the particles are, the higher glass content it has. However, the fly ashes in the third field of 300 MW had 1.5% lower glass content but higher specific gravity than those in the second field of 600 MW. Therefore, the shell wall thickness of fly ashes may not greatly affect the specific gravity. In hollow fly ashes, the finer the particles are, the more likely the volume of closed pores will decrease. Figs. 4 and 5 show the relationship between specific gravity and fineness. Specific gravity and Blaine specific surface area represent a direct relationship and an exponential correlation with residue on 45-μm sieve shown. Therefore, the most important factors affecting specific gravity may be the content of closed pores.

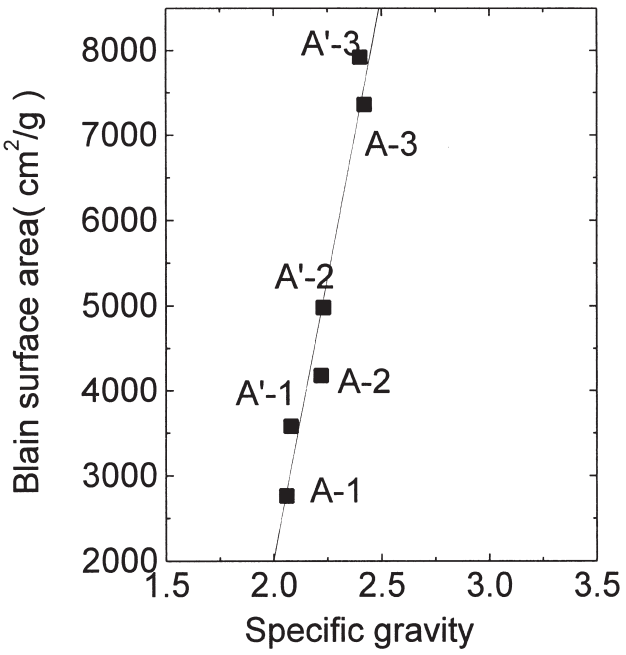

Fig. 4. The relationship between Blaine specific area and specific gravity.

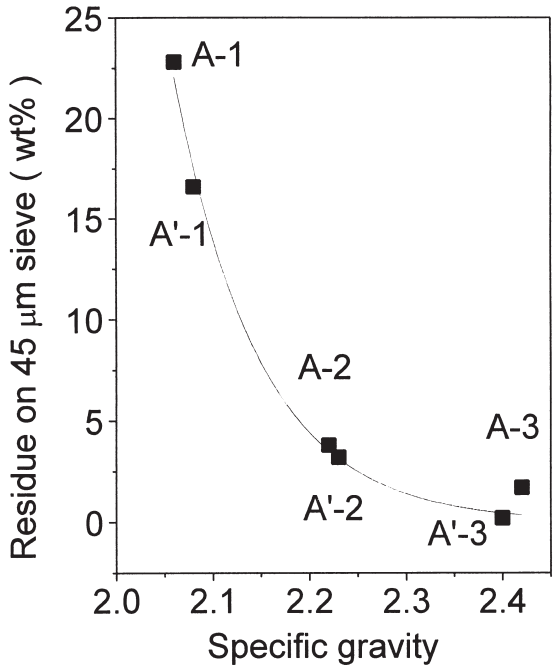

Fig. 5. The relationship between specific gravity and residue on 45-μm sieve.

3.5. The tone of colors of fly ashes

The overall color of fly ashes is gray. The fly ashes indicate dark gray, medium gray, light gray by the Munsell color chart [9] going from the first field to the third one. Fly ashes collected from the same location represented the same tone of color, regardless of the boiler load. The color of fly ash is reported to depend on the amount of Fe_2O_3 and unburned carbon [2]. However, there were no such trends in this experiment. Moreover, Fe_2O_3 content had a similar value of 4.2 to 4.8% and carbon content had value as low as 0.3 to 1.5%. A-1 and A′-1 had largest most differences in amount compared to Fe_2O_3 and carbon content among all fly ashes represented by the same tone of color. Presumably, in fly ashes produced from the same coal, the smaller the size of particles becomes, the brighter they become.

3.6. Reactivity with $Ca(OH)_2$

Fig. 6 shows the relation between the aging time for fly ashes at 40°C and the reactivity with $Ca(OH)_2$. The amount of reaction with $Ca(OH)_2$ increased with aging time, but after 28 days there was virtually no change. The reactivity of fly ashes with $Ca(OH)_2$ increased going from the first field to the third one, and fly ashes collected from the same location had slightly better reactivity with $Ca(OH)_2$ at 300-MW load than at 600-MW load. Factors affecting the pozzolanic reactivity may include fineness and glass content. The reactivity with $Ca(OH)_2$ increases with content of finer particles

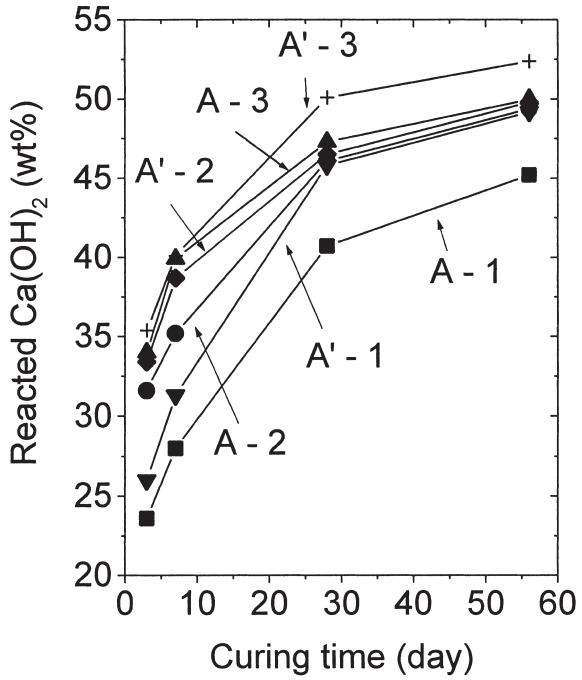

Fig. 6. Amount of reacted $Ca(OH)_2$ with curing time at 40°C.

in the same running conditions of boiler. If the fly ashes in the same field of 600 and 300 MW were compared to each other, the former had higher glass content than that of 300 MW, but the latter had finer particles than that of 600 MW. Thus, the initial pozzolanic reactivity of fly ashes was more affected by fineness than by glass content.

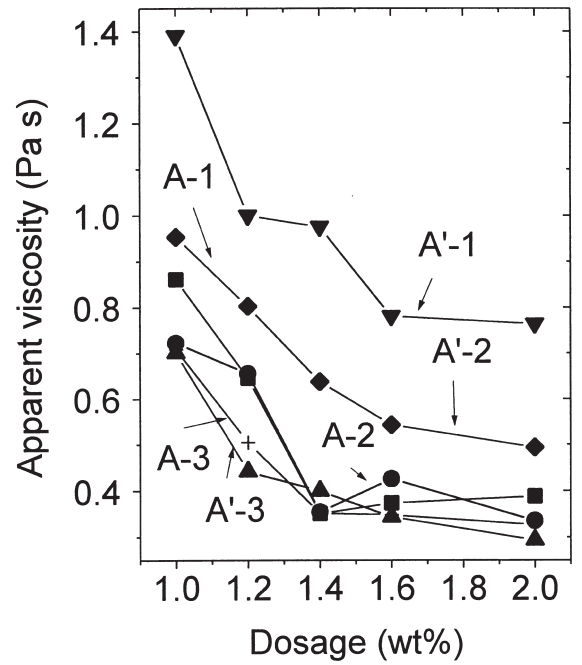

Fig. 7. The influence of dosage of superplasticizer on the apparent viscosity of paste with fly ash.

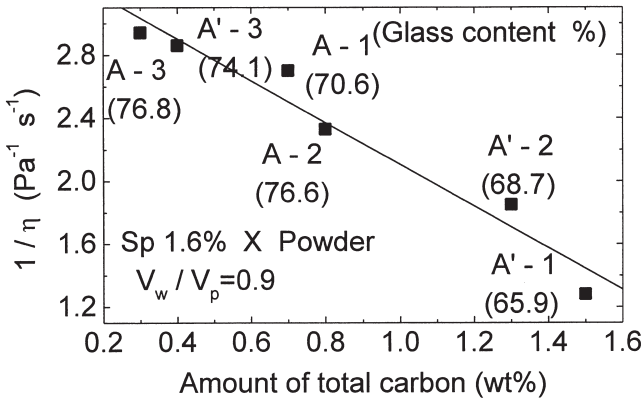

Fig. 8. The relationship between amount of total carbon and 1/η of pastes (η = apparent viscosity).

3.7. Evaluation of apparent viscosity

Fig. 7 shows the relation between the apparent viscosity of cement paste with 20 vol% of fly ashes and the amount of addition of superplasticizer. With up to 1.6% of superplasticizer, the apparent viscosity of paste decreased regardless of the kinds of fly ashes. For more admixture, there was no change. This may be because the amount of admixture adsorbed on particles reached saturation around 1.6 wt% of superplasticizer. The apparent viscosity is represented as $\eta = \tau/\gamma$ (where τ is shear stress and γ is shear velocity) and counteracts to the reverse value of shear velocity generated under certain shear stress. From the standpoint of fluidity, the evaluation by $1/\eta$, the shear velocity itself is important rather than η counteracting to the reverse value of shear velocity. Fig. 8 represents the relationship between carbon content and the reverse value of apparent viscosity in 1.6%, where the addition of admixture is saturated. The value $1/\eta$ linearly decreases as the carbon content increases.

4. Conclusions

The results obtained in this experiment can be stated as follows:

1. Regardless of boiler running conditions, the fly ashes collected increased in fineness, specific gravity, and glass content going from the first collector field to the third field, but SiO_2 content was decreased.
2. When the boiler is operated at full-operating load (600 MW) in comparison with operating at half load (300 MW), the glass content was greater, but the Blaine specific surface area and carbon content were lower.
3. Initial reactivity of fly ashes at 40°C with $Ca(OH)_2$ was more affected by fineness than by glass content.
4. In cement paste of 20 vol% of fly ashes, the apparent viscosity decreased with superplasticizer addition but revealed a constant value at 1.6% of superplasticizer.

There was a linear correlation between carbon content and fluidity at this constant saturated condition.

References

[1] R.T. Hemming, E.E. Berry, On the glass in coal fly ashes: Recent advances, Mat Res Soc Symp Proc 113 (1988) 3–38.
[2] L. Alexanders, H.P. Klug, Basic aspects of X-ray absorption, Anal Chem 20 (1948) 886–889.
[3] M. Roode, E. Douglas, R.T. Hemmings, X-ray diffraction measurement of glass content in fly ashes and slags, Cem Concr Res 17 (1987) 183–197.
[4] T. Tanosaki, K. Nozaki, K. Tanigawa, S. Ashiyahara, K. Manabe, Characterization of Japanese coal ash in recent years, J Res of Chichibu Onoda Cem Co 46 (1995) 104–125.
[5] G.J. MacCarthy, D.M. Johansen, S.T. Thedchanamoorthy, S.J. Steinwand, K.D. Swansong, Characterization of North American lignite fly ashes II. XRD mineralogy, Mat Res Soc Symp 113 (1988) 99–105.
[6] S. Diamond, On the glass present in low-calcium and in high-calcium fly ashes, Cem Concr Res 13 (1983) 459–464.
[7] S.W. Frieman, L.L. Hench, Further analysis of glass crystallization kinetics, J Am Ceram Soc 52 (1969) 111–115.
[8] D. Kunii, O. Levenspiel, Fludization Engineering, Butterworth-Heineman Series in Chemical Engineering, Academic Press, Inc., New York, 1944.
[9] A.H. Munsell, The Munsell Atlas of Color, Mumsell Color Co., Baltimore, 1929.